Dalton Transactions

Mononuclear Fe(III) Schiff Base Antipyrine Complexes for Catalytic Hydrogen Generation

Journal:	*Dalton Transactions*
Manuscript ID	DT-COM-06-2024-001876.R2
Article Type:	Communication
Date Submitted by the Author:	30-Aug-2024
Complete List of Authors:	Cropley, Jessica; William & Mary, Chemistry Mitchell, Amanda; William & Mary, Chemistry Fritsch, Nicole; William & Mary Ho, Marissa; William & Mary, Chemistry Wells, Timothy; William & Mary, Chemistry Reynolds, Todd; William & Mary, Department of Chemistry Brennessel, William; University of Rochester, Department of Chemistry McNamara, William; William & Mary, Chemistry

COMMUNICATION

Mononuclear Fe(III) Schiff Base Antipyrine Complexes for Catalytic Hydrogen Generation

Received 00th January 20xx,
Accepted 00th January 20xx

DOI: 10.1039/x0xx00000x

Jessica D. Cropely, [a] Amanda C. Mitchell, [a] Nicole A. Fritsch, [a] Marissa Ho, [a] Timothy D. Wells, [a] Todd M. Reynolds, [a] William W. Brennessel, [b] and William R. McNamara [a]

Mononuclear Fe(III) complexes containing an antipyrine Schiff Base ligand were prepared and fully characterized, demonstrating a planar tetradentate coordination geometry. These complexes were found to be active for the Hydrogen Evolution Reaction. Catalysis occurs at -1.4 V vs. Fc^+/Fc, with an overpotential of 700 mV. The complexes are active electrocatalyst with a turnover frequency of 700 s^{-1}. Furthermore, when paired with a chromophore and sacrificial donor, the complexes are active photocatalysts demonstrating > 1,700 turnovers during 40 hours of irradiation with a quantum yield of up to 5.4%. The catalysts have also been found to operate in natural water samples of varying salinity.

With rising greenhouse gas emissions due to the combustion of fossil fuels, the development and use of renewable energy sources is critical.[1] Artificial Photosynthesis (AP) focuses on splitting water using photons. In AP, water can be oxidized to O_2 and coupled with either carbon dioxide reduction or the evolution of dihydrogen. The hydrogen evolution reaction (HER) focuses on the reductive side of AP, with the goal of producing carbon-neutral energy in the form of hydrogen gas. The H_2 gas can be either combusted directly or used in hydrogen fuel cells.[2] In order to fully realize this goal, proton reduction catalysts made from earth abundant materials must be developed.[1] Since iron is the most abundant transition metal, it is of interest to explore the use of iron in complexes that are highly active and stable for hydrogen evolution.

Platinum has been traditionally viewed as a benchmark electrocatalyst for HER due to its high activity, low overpotential, and robustness.[3] However, the low abundance and high cost of Pt limits the widespread applicability of such catalysts.[4] In order to circumvent this limitation, first row transition metals such as Co and Ni have been studied extensively for use as proton reduction catalysts and show great promise for the HER.[5] Taking a bio-inspired approach, molecular catalysts have also been developed that mimic hydrogenase enzymes. These Fe and Ni catalysts show high activity, but are often active with the addition of organic acids in nonaqueous solvents.[6] Therefore, it is of interest to develop catalysts that are active, robust, and operate in aqueous solutions.[7]

The use of redox-active ligands in catalysis is well-established and can allow for multi-electron processes using first-row transition metals.[8] Previous studies in our group described a nickel catalyst with a redox-active bis-dithiocarbazate ligand that was active in water for the HER.[9] Furthermore, the versatility of this catalyst was seen when it was paired with molecular chromophores for photocatalytic hydrogen generation. With this promising result, we seek to develop iron catalysts containing redox active ligands for hydrogen generation.

For widespread applicability, it is our goal to develop catalysts that contain ligands that can be accessed through inexpensive precursors in good yield. Schiff base ligands are particularly attractive owing to their multidentate nature and facile synthesis. Herein we report an iron catalyst containing a Schiff base, N,N'-bis(4-antipyrlmethylidene)ethylenediamine (Figure 1) ligand, that is active for both the photocatalytic and electrocatalytic generation of hydrogen. The resulting catalyst operates at a 700 mV overpotential and photocatalytic systems achieve turnovers > 1,700. Furthermore, these photocatalytic systems operate with natural water samples of varying salinity, underscoring the robust nature of the catalyst.

[a] *Department of Chemistry, College of William and Mary, 540 Landrum Drive, Williamsburg, VA 23185.*
[b] *Department of Chemistry, University of Rochester, 120 Trustee Road, Rochester, NY 14627.*
† Footnotes relating to the title and/or authors should appear here.
Electronic Supplementary Information (ESI) available: [details of any supplementary information available should be included here]. See DOI: 10.1039/x0xx00000x

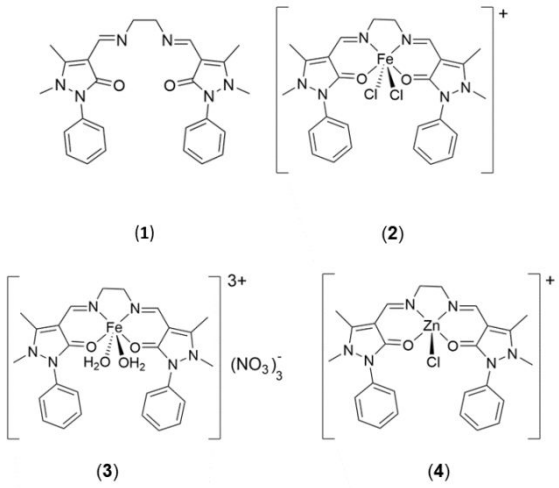

Figure 1. Top Left: N,N'- bis(4-antipyrlmethylidene)-ethylenediamine ligand (**1**); Top Right: [Fe(**1**)Cl_2]Cl, (**2**); Bottom Left: [Fe(**1**)$(OH)_2$]$(NO_3)_3$, (**2**); Bottom Right: [Zn(**1**)Cl]Cl, (**4**).

The N,N'-bis(4-antipyrlmethylidene)-ethylenediamine (BAME, **1**) ligand was of interest due to the similarity to well-established salen ligands, and potential ONNO tetradentate coordination geometry as a neutral donor ligand.[10] Although ligand **1** has been previously reported, iron complexes of this ligand have not been isolated and fully characterized.[10,11] To this end, the ligand was synthesized according to a modified literature procedure.[10] A solution of ethylene diamine in ethyl acetate (0.5 equivalents) was added dropwise to a solution of 4-antipyryine carboxaldehyde (1 equivalent) in ethyl acetate. The resulting solution was refluxed for 4 hours, allowed to cool to room temperature, and filtered to give the product as a white solid (66% yield).

The iron chloride salt was of interest owing to the established activity of iron polypyridyl complexes with chloro ligands.[12] A solution of $FeCl_3 \cdot 6H_2O$ in acetone was added dropwise to a solution of **1** in acetone and refluxed for 4 hours. During this time, a brick red precipitate formed and was collected via vacuum filtration. The red precipitate was dried further under vacuum to give **2** in a 96% yield. Crystals suitable for X-ray diffraction were grown through diffusion of the dissolved complex in MeOH into ethyl acetate.

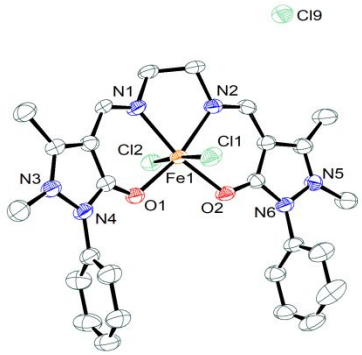

Figure 2. ORTEP Diagram of **2** with Fe (orange), O (red), N (blue), Cl (green), and C (gray). Hydrogen atoms omitted for clarity.

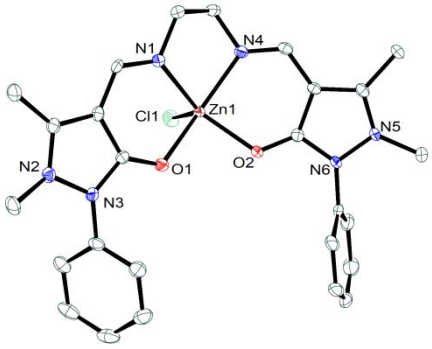

Figure 3. ORTEP Diagram of **4** with Zn (brown), O (red), N (blue), Cl (green), and C (gray). Hydrogen atoms and outer sphere Cl^- were omitted for clarity.

Ligand **1** was found to coordinate Fe(III) to give mononuclear complex **2**. The iron center shows distorted octahedral geometry, with all Fe-L bonds to **1** between 2.0 and 2.1 Å, and Fe-Cl bonds slightly longer at 2.3-2.4 Å. The O(1)-Fe-O(2) and N(2)-Fe-N(1) bond angles are 102.9° and 76.8°, respectively, with all other angles about Fe within 10% difference from the expected angles of 180° and 90° (Figure 2). The bond lengths of 1.286(6) and 1.269(6) Å are consistent with C=O double bond character for the coordinated ligand, suggesting neutral donation from **1**.

To probe any potential redox activity of the ligand, a Zn analogue was synthesized as a point of comparison. A solution of $ZnCl_2$ in acetone was added dropwise to a solution of **1** in acetone. The resulting solution was refluxed for 4 hours and allowed to cool to room temperature. The light-yellow zinc complex, **4**, precipitated out of solution and was collected via vacuum filtration (71 % yield). Crystals suitable for X-ray diffraction were obtained by slow diffusion of diethyl ether into a solution of **4** in MeOH. The resulting Zn complex shows a square pyramidal coordination geometry with ligand **1** acting as a tetradentate ONNO L4 donor similar to what was observed for the iron complex. This is confirmed by C-O bond distances of 1.257(4) and 1.263(4) Å, which demonstrate the double bond character between C and O, suggesting neutral donation to the Zn center from **1**.

Cyclic Voltammograms of **2** show a reversible redox couple at -0.4 V vs. Fc^+/Fc, corresponding to a the Fe(III/II) redox couple (Figure 4). Upon addition of a proton source, trifluoroacetic acid (TFA), a catalytic wave is observed with an onset potential of -1.4 V vs. Fc^+/Fc, corresponding to catalytic hydrogen generation with an overpotential of 700 mV and an i_c/i_p = 5.3 (see supporting information). Hydrogen generation was confirmed using controlled potential coulometry with an

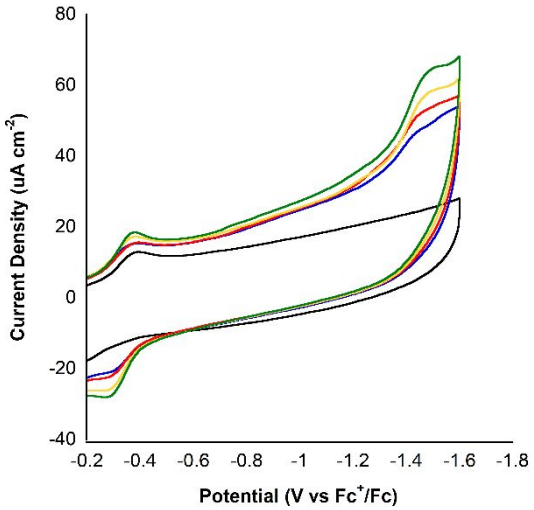

Figure 4. CVs of **2** with no acid (black), 0.44 mM (blue), 0.88 mM (red), 1.32 mM (yellow) and 1.76 mM (green) TFA. These experiments were performed in CH_3CN with 0.1M $TBAPF_6$ and 0.1 mM **2** with scan rate = 200 mV/s.

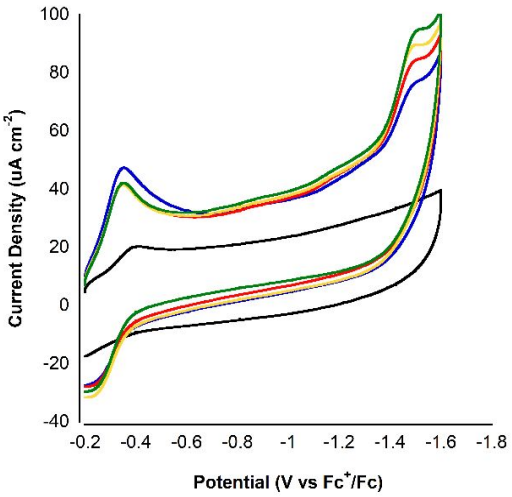

Figure 5. CVs of **3** with no acid (black), 0.44 mM (blue), 0.88 mM (red), 1.32 mM (yellow) and 1.76 mM (green) TFA. These experiments were performed in CH_3CN with 0.1M $TBAPF_6$ and 0.09 mM **3** with scan rate = 200 mV/s.

applied voltage of -1.5 V vs. Fc^+/Fc with a faradaic yield of 99% (see supporting information). With a catalytic wave that is 1 V more cathodic than the Fe(III/II) redox couple, it is hypothesized that the electrochemical mechanism proceeds through a reduction (E) followed by subsequent chemical steps (C) and an additional electrochemical step (E), resulting in either an ECCE or ECEC mechanism for hydrogen generation. A linear relationship between catalytic current and both proton and catalyst concentration is observed, suggesting the reaction is first order in catalyst and second order with respect to $[H^+]$ (see supporting information).

It should be noted that complex **2** contains a chloride counteranion. The effects of counteranions in hydrogen generation have been examined for Ni complexes, showing that chloride counteranions demonstrate lower activity than those with non-coordinating anions.[14] To investigate this effect, the diaquo analogue was obtained as a nitrate salt (**3**). CVs of **3** reveal a Fe(III/II) redox couple at -0.4 V vs. Fc^+/Fc, with a catalytic wave observed with an onset potential of -1.4 V vs. Fc^+/Fc upon addition of TFA (Figure 5) and an i_c/i_p = 4.8. Complex **3** operates at similar potentials with comparable activity, suggesting that dissociation of a chloro ligand to yield a vacant site likely plays a role in the activity of **2**. With complex **2** and **3** showing promising catalytic activity, it was of interest to probe whether the ligand could be participating in the chemical steps of catalysis.

With Zn being redox inactive within these potential ranges, the Zn analogue (**4**) was investigated using cyclic voltammetry. Under the same potential range, no metal- or ligand-based redox events were observed for complex **4** (Figure 6, black). Upon addition of trifluoroacetic acid, protonation of the ligand is observed at -1.4 V vs. Fc^+/Fc (Figure 6, red). This redox event is comparable to what is observed for acid additions for the ligand alone (see supporting information). Controlled potential coulometry with an applied voltage of -1.5 V vs. Fc^+/Fc was performed and no hydrogen generation was observed. This indicates that while ligand protonation is observed for **4**, no hydrogen is generated catalytically for the zinc complex. Therefore, it is possible for the protonation of the ligand to play a role in catalysis.

To further probe the potential role of ligand protonation, acid addition studies were performed spanning a wide pKa range (trifluoroacetic acid, pKa = 12.65; salicylic acid, pKa = 16.7;

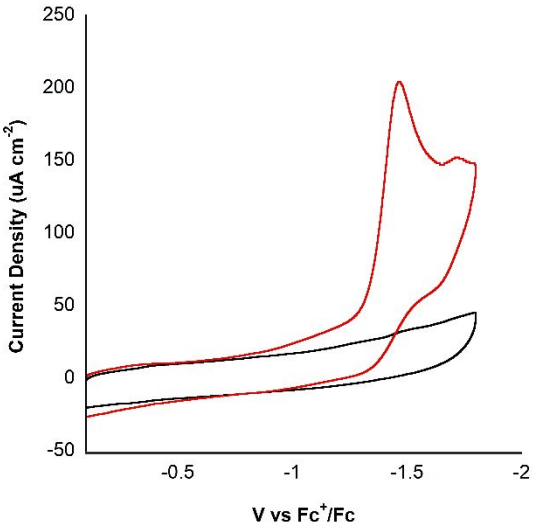

Figure 6. CVs of **4** with no acid (black) and after the addition of 0.44 mM acid (red). These experiments were performed in CH_3CN with 0.1M $TBAPF_6$ and 0.1 mM **4** with scan rate = 200 mV/s.

acetic acid, pKa = 23.51; and phenol, pKa = 29.14). Phenol and acetic acid do not protonate the ligand and no catalytic response is observed upon addition of these acids to the iron complexes (see supporting information). Salicylic acid protonates the ligand; however, no catalytic response is observed upon addition of salicylic acid to the iron complexes. One possible mechanism includes: reduction of the complex to Fe(II), followed by protonation of the ligand, and subsequent reduction of the complex to Fe(I) where a proton is shuttled from the ligand to form an Fe(III)H intermediate. This intermediate could then react directly with acid to liberate H_2, or through bimetallic elimination of H_2. A similar mechanism where the ligand is doubly protonated is also possible.

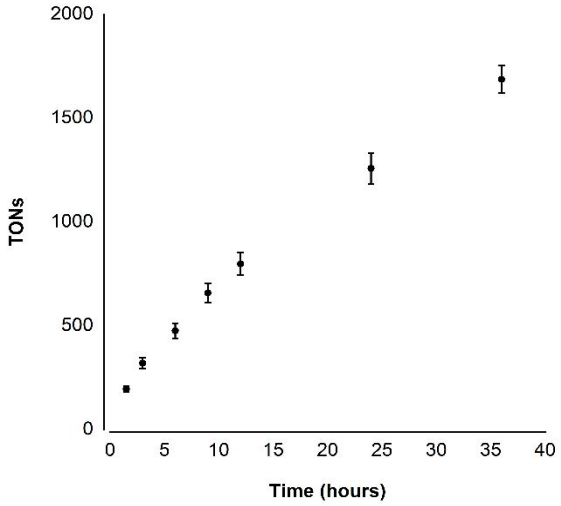

Figure 7. Hydrogen Generation observed for 7.5 µM **2** when paired with 1.8 mM Fl and 5% TEA in 1:1 EtOH:Water.

Following the observed electrocatalytic activity of **2** and **3** for the HER, it was of interest to explore the viability of this complex in a photocatalytic system. To this end, the iron complexes were paired with a chromophore, fluorescein, that is known to reduce catalysts that operate at similar redox potentials, and triethylamine as a sacrificial donor.[12] Upon irradiation with visible light (λ = 520 nm, 0.12 W), hydrogen evolution was observed for solutions containing complexes **2-3**, Fl, and 5% TEA in a 1:1 water:ethanol mixture (Figure 7). The optimal catalyst concentration was found to be 7.5 µM for each catalyst (see supporting information). The optimal [Fl] was found to be 1.8 mM for systems containing **2-3** (see supporting information). The system is also most active when pH = 12.5, which is consistent with other photocatalytic systems containing Fl and TEA, where TEA is a better electron donor at higher pH.[12] To confirm the activity of **2**, control experiments replacing **2** with the ligand only, $FeCl_3$ only, and **4** only failed to produce hydrogen gas.

As interest in a "green hydrogen economy" grows, several challenges present themselves when determining scalability of systems for hydrogen generation: hydrogen storage, limitations of current hydrogen fuel cells, and also sources of water remain a challenge.[13] In a green hydrogen economy where hydrogen gas is produced through electrolysis, it is projected that more fresh water would be required than is currently utilized in our fossil fuel based strategies.[13] Furthermore, reliable access to fresh water is not available in every global location. To this end, hydrogen production from seawater is an active area of research. However, potential limitations include the evolution of chlorine and oxygen gas at the anode.[15] Therefore, it was of interest to determine if the photocatalytic system featuring complex **2** would be active with local water samples of varying salinity.

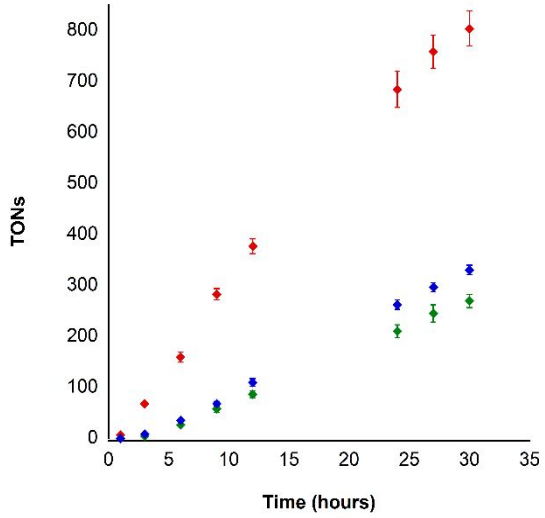

Figure 8. Hydrogen generation observed for 7.5 µM **2** when paired with 1.8 mM Fl and 5% TEA in 1:1 EtOH:Water when water used is fresh lake water (red), brackish bay water (green) and seawater (blue).

To this end, local water samples of fresh water (< 0.5 ppt salinity), brackish/tidal water (24 ppt salinity), as well as ocean water (34 ppt salinity) were examined as potential water sources.[16] The local water samples were obtained and filtered through celite to remove any solid contaminants. The water was then combined with ethanol to produce a 1:1 EtOH:water mixture to ensure solubility of catalyst and chromophore. The resulting catalyst, chromophore, and TEA solutions were irradiated with visible light and hydrogen generation was observed for each sample (Figure 8). Unsurprisingly, hydrogen generation was observed with fresh lake water. Interestingly, hydrogen generation was also observed when using brackish and saltwater. The lower activity observed for brackish and bay water matches what is observed for control experiments with varying NaCl concentrations (see supporting information), which agrees with the observed lower activity of nickel complexes with chloride anions.[14] With activity in a wide range of natural water samples, this result underscores the robust nature of the catalyst and shows the potential of using water of varying salinity for photocatalytic hydrogen generation.

Conclusions

In summary, we have found that an iron complexes of the Schiff base, N,N'-bis(4-antipyrlmethylidene)-ethylenediamine are readily synthesized in very good yield, providing a tetradentate coordination geometry. X-ray crystallography revealed significant C=O character in the ligand, suggesting that it binds to Fe and Zn as a tetradentate neutral donor ligand. The synthesis of an analogous zinc compound shows that protonation of the ligand is possible under catalytic conditions and may play a pivotal role in catalysis. Complex **2** and **3** operate with an overpotential of 700 mV with an i_c/i_p of 5.3, and 4.8, respectively. When combined with a fluorescein chromophore and TEA sacrificial electron donor, the catalyst was active photocatalytically, exhibiting over 1,700 TON over 40 hours and a quantum yield of 5.4% for **2**, and 2.9 % for **3**. Activity in natural water sources shows **2**-**3** to be robust photocatalysts capable of generating H_2 from natural water.

Author Contributions

JDC, ACM, NAF, MH, TDW carried out syntheses, characterization, and electrochemical experiments. WWB, and TMR acquired the X-ray crystallographic characterization. WRM has supervised and administered the project.

Conflicts of interest

There are no conflicts to declare.

Notes and references

1 (a) N. S. Lewis and D. G. Nocera, *Proc. Natl. Acad. Sci*., 2006, **103**, 15729. (b) R. Eisenberg, *Science*, 2009, **324**, 44. (c) A. Hossain, K. Sakthipandi, A. K. M. Atique Ullah and S. Roy, *Nano-Micro Lett.*, 2019, **11**, 103. (d) B. Zhang and L. Sun, *Chem. Soc. Rev.*, 2019, **48**, 2216–2264.

2 D. L. Dubois, *Inorg. Chem.*, 2014, **53**, 3935-3960.

3 (a) C. C. L. McCrory, S. Jung, I. M. Ferrer, S. M. Chatman, J. C. Peters and T. F. Jaramillo, *J. Am. Chem. Soc.*, 2015, **137**, 4347-4357. (b) E. S. Rountree, B. D. McCarthy, T. T. Eisenhart and J. L. Dempsey, *Inorg. Chem.*, 2014, **53**, 9983–10002.

4 (a) P. C. K. Vesborg and T. F. Jaramillo, *RSC Adv.*, 2012, **2**, 7933–7947. (b) M. Chatenet, B. G. Pollet, D. R. Dekel, F. Dionigi, J. Deseure, P. Millet, R. D. Braatz, M. Z. Bazant, M. Eikerling, I. Staffell, P. Balcombe, Y. Shao-Horn and H. Schäfer, *Chem. Soc. Rev.*, 2022, **51**, 4583–4762.

5 (a) P. Connolly and J. H. Espenson, *Inorg. Chem.*, 1986, **25**, 2684. (b) X. Hu, B. S. Brunschwig and J. C. Peters, *J. Am. Chem. Soc.*, 2007, **129**, 8988. (c) J. L. Dempsey, B. S. Brunschwig, J. R. Winkler and H. B. Gray, *Acc. Chem. Res.*, 2009, **42**, 1995. (d) C. Baffert, V. Artero and M. Fontecave, *Inorg. Chem.*, 2007, **46**, 1817. (e) M. Razavet, V. Artero and M. Fontecave, *Inorg. Chem.*, 2005, **44**, 4786. (f) P. A. Jacques, V. Artero, J. Pecaut and M. Fontecave, *Proc. Nat. Acad. Sci. U. S. A.*, 2009, **106**, 20627. (g) X. L. Hu, B. M. Cossairt, B. S. Brunschwig, N. S. Lewis and J. C. Peters, *Chem. Commun.*, 2005, 4723-4725. (h) D. L. DuBois, *Inorg. Chem.*, 2014, **53**, 3935-3960. (i) R. M. Bullock, A. M. Appel and M. L. Helm, *Chem. Commun.*, 2014, **50**, 3125-3143. (j) A. D. Wilson, R. H. Newell, M. J. McNevin, J. T. Muckerman, M. Rakowski Dubois and D. L. Dubois, *J. Am. Chem. Soc.*, 2006, **128**, 358-366. (k) M. D. Kärkäs, O. Verho, E. V. Johnston, B. Åkermark, *Chem. Rev.*, 2014, **114**, 11863–12001. (l) F. Lucarini, J. Fize, A. Morozan, F. Droghetti, E. Solari, R. Scopelliti, M. Marazzi, M. Natali, M. Pastore, V. Artero and A. Ruggi, *Sustainable Energy Fuels*, 2023, **7**, 3384–3394. (m) M. B. Brands and J. N. H. Reek, *Inorg. Chem.*, 2024, **63**, 8484–8492. (n) D. Dolui, S. Khandelwal, P. Majumder and A. Dutta, *Chem. Commun.*, 2020, **56**, 8166–8181. (o) N. Kaeffer, M. Chavarot-Kerlidou and V. Artero, *Acc. Chem. Res.*, 2015, **48**, 1286–1295. (p) E. S. Wiedner, A. M. Appel, S. Raugei, W. J. Shaw and R. M. Bullock, *Chem. Rev.*, 2022, **122**, 12427–12474.

6 (a) E. Garcin, X. Vernede, E. C. Hatchikian, A. Volbeda, M. Frey and J. C. Fontecilla-Camps, *Structure*, 1999, **7**, 557-566. (b) J. W. Peters, W. N. Lanzilotta, B. J. Lemon and L. C. Seefeldt, *Science*, 1998, **282**, 1853-1858. (c) X. Zhao, I. P. Georgakaki, M. L. Miller, J. C. Yarbrough and M. Y. Darensbourg, *J. Am. Chem. Soc.*, 2001, **123**, 9710-9711. (d) G. A. N. Felton, R. S. Glass, D. L. Lichtenberger and D. H. Evans, *Inorg. Chem.*, 2006, **45**, 9181-9184. (e) F. Gloaguen, J. D. Lawrence and T. B. Rauchfuss, *J. Am. Chem. Soc.*, 2001, **123**, 9476-9477. (f) M. E. Carroll, B. E. Barton, T. B. Rauchfuss and P. J. Carroll, *J. Am. Chem. Soc.*, 2012, **134**, 18843-18852. (g) M. Alfano and C. Cavazza, *Protein Science*, 2020, **29**, 1071–1089. (h) W. Lubitz, H. Ogata, O. Rüdiger and E. Reijerse, *Chem. Rev.*, 2014, **114**, 4081–4148. (i) S. Aguado, L. Casarrubios, C. Ramírez De Arellano and M. A. Sierra, *RSC Adv.*, 2020, **10**, 29855–29867. (j) D. Schilter, J. M. Camara, M. T. Huynh, S. Hammes-Schiffer and T. B. Rauchfuss, *Chem. Rev.*, 2016, **116**, 8693–8749.

7 (a) A. D. Nguyen, M. D. Rail, M. Shanmugam, J. C. Fettinger and L. A. Berben, *Inorg. Chem.*, 2013, **52**, 12847-12854. (b) M. L. Singleton, J. H. Reibenspies and M. Y. Darensbourg, *J. Am. Chem. Soc.*, 2010, **132**, 8870. (c) M. L. Singleton, D. J. Crouthers, R. P. Duttweiler, J. H. Reibenspeis and M. Y. Darensbourg, *Inorg. Chem.*, 2011, **50**, 5015. (d) F. Quentel, G. Passard and F. Gloaguen, *Chem. Eur. J.*, 2012, **18**, 13473. (e) K. E. Dalle, J. Warnan, J. J. Leung, B. Reuillard, I. S. Karmel and E. Reisner, *Chem. Rev.*, 2019, **119**, 2752–2875. (f) Z. Xiao, W. Zhong and X. Liu, *Dalton Trans.*, 2022, **51**, 40–47. (g) C. Esmieu, P. Raleiras and G. Berggren, *Sustainable Energy Fuels*, 2018, **2**, 724–750.

8 (a) O. R. Luca and R. H. Crabtree, *Chem. Soc. Rev.*, 2013, **42**, 1440–1459. (b) W. R. McNamara, Z. Han, P. J. Alperin, W. W. Brennessel, P. L. Holland and R. Eisenberg, *J. Am. Chem. Soc.*, 2011, **133**, 15368-15371. (c) L. Leone, G. Sgueglia, S. La Gatta, M. Chino, F. Nastri and A. Lombardi, *IJMS*, 2023, **24**, 8605. (d) E. Peris and R. H. Crabtree, *Chem. Soc. Rev.*, 2018, **47**, 1959–1968.

9 C. F. Wise, D. Liu, K. J. Mayer, P. M. Crossland, C. L. Hartley and W. R. McNamara, *Dalton Trans.*, 2015, **44**, 14265–14271.

10 S. Joseph and P. K. Radhakrishnan, *Polyhedron*, 1999, **18**, 1881-1884.

11 M. T. Madhu and P. K. Radhakrishnan, *Synthesis and Reactivity in Inorganic and Metal-Organic Chemistry*, 2001, **31**, 1663-1673.

12 C. L. Hartley, R. J. DiRisio, M. E. Screen, K. J. Mayer and W. R. McNamara, *Inorg. Chem.*, 2016, **55**, 8865-8870.

13 R. R. Beswick, A. M. Oliveira and Y. Yan, *ACS Energy Letters*, 2021, **6**, 3167-3169.

14 T. Kato, R. Tatematsu, K. Nakao, Inomata, T., Ozawa, T., and H. Masuda, *Inorg. Chem.* 2021, **60**, 7670-7679.

15 A.-M.A El-Bassuoni, J. W. Sheffield and T. N. Vezi-roglu, *Int. J. Hydrogen. Energy.*, 1982, **7**, 919-923.

16 Virginia Institute of Marine Science, Chesapeake Bay Environmental Forecast System, https://www.vims.edu/research/products/cbefs/ (Accessed 6/27/2024)

Data Availability Statement

The data supporting this communication have been included as part of the supporting information.

All data is available upon request.

Crystallographic data for [2], [3], and [4] have been deposited at the CCDC under 2320558, 2353558, and 2320559, respectively. This data can be obtained from https://www.ccdc.cam.ac.uk/